

The radio loud narrow-line quasar SDSS J172206.03+565451.6

Stefanie Komossa, Wolfgang Voges, Hans-Martin Adorf

*Max-Planck-Institut für extraterrestrische Physik, Postfach 1312, 85741 Garching,
Germany; skomossa@mpe.mpg.de*

and

Dawei Xu

*National Astronomical Observatories, Chinese Academy of Science, A20 Datun Road,
Chaoyang District, Beijing 100012, China*

and

Smita Mathur

*Department of Astronomy, The Ohio State University, 140 West 18th Avenue, Columbus,
OH 43210, USA*

and

Scott F. Anderson

Department of Astronomy, University of Washington, Box 351580, Seattle, WA 98195

ABSTRACT

We report identification of the radio loud narrow-line quasar SDSS J172206.03+565451.6 which we found in the course of a search for radio loud narrow-line Active Galactic Nuclei (AGN). SDSS J172206.03+565451.6 is only the ~ 4 th securely identified radio loud narrow-line quasar and the second-most radio loudest with a radio index $R_{1.4} \approx 100 - 700$. Its black hole mass, $M_{\text{BH}} \simeq (2 - 3) \times 10^7 M_{\odot}$ estimated from $\text{H}\beta$ line width and 5100\AA luminosity, is unusually small given its radio loudness, and the combination of mass and radio index puts SDSS J172206.03+565451.6 in a scarcely populated region of $M_{\text{BH}}-R$ diagrams. SDSS J172206.03+565451.6 is a classical Narrow-Line Seyfert 1-type object with $\text{FWHM}_{\text{H}\beta} \simeq 1490 \text{ km/s}$, an intensity ratio of $[\text{OIII}]/\text{H}\beta \simeq 0.7$ and FeII emission complexes with $\text{FeII}\lambda 4570/\text{H}\beta \simeq 0.7$. The ionization parameter of its narrow-line region, estimated from the line ratio $[\text{OII}]/[\text{OIII}]$, is similar to

Seyferts and its high ratio of $[\text{NeV}]/[\text{NeIII}]$ indicates a strong EUV to soft-X-ray excess. We advertise the combined usage of $[\text{OII}]/[\text{OIII}]$ and $[\text{NeV}]/[\text{NeIII}]$ diagrams as a useful diagnostic tool to estimate ionization parameters and to constrain the EUV–soft-X-ray continuum shape relatively independent from other parameters.

Subject headings: quasars: individual (SDSS J172206.03+565451.6) – quasars: emission lines – quasars: general – X-rays: galaxies – radio continuum: galaxies

1. Introduction

Narrow-line Seyfert 1 (NLS1) galaxies were identified by Osterbrock & Pogge (1985) as a subgroup of Seyfert galaxies with small widths of the broad Balmer lines ($\text{FWHM}_{\text{H}\beta} < 2000$ km/s). Correlation analyses have shown that $\text{H}\beta$ line width is anti-correlated with the strength of $\text{FeII}/\text{H}\beta$ emission complexes and correlated with the strength of $[\text{OIII}]\lambda 5007$ (Boroson & Green 1992). The study of NLS1s and correlations among their properties is expected to hold important clues on the physical processes in the central region of AGN (see Veron-Cetty & Veron 2000 for a general AGN review). There is increasing evidence that most NLS1s accrete close to or at the Eddington limit (e.g., Boroson & Green 1992, Pounds et al. 1995, Marziani et al. 2001, Simkin & Roychowdhury 2003, Xu et al. 2003, Wang & Netzer 2003, Grupe 2004, Collin & Kawaguchi 2004) and that they follow a different black hole mass – velocity dispersion ($M_{\text{BH}} - \sigma$) relation than broad line Seyfert 1 galaxies (e.g., Mathur 2001, Grupe & Mathur 2004, Botte et al. 2004, Mathur & Grupe 2005).

While the optical and X-ray properties of NLS1s were explored intensively in the last decade, relatively little is known about their radio properties (Ulvestad et al 1995, Moran 2000, Greene et al. 2005). In particular, only a few radio loud NLS1s and narrow-line quasars (NLQSOs) have been identified so far¹, namely three detections and one or two candidates. PKS0558-504 (Remillard et al. 1986, Siebert et al. 1999), RXJ0134-4258 (Grupe et al. 2000), and SDSS J094857.3+002225 (Zhou et al. 2003) all match optical classification criteria of NLQSOs and show radio indices exceeding $R = 10$, SDSS J094857.3+002225 even has $R > 1000$. PKS 2004-447 (Oshlack et al. 2001) may be a non-typical NLS1 or possibly a narrow-line radio galaxy (Zhou et al. 2003) and is very radio loud. RGB J0044+193 (Siebert et al. 1999) is radio quiet most of the time (Maccarone et al. 2005), but may have been radio loud at the epoch of the 87GB survey.

¹there are preliminary reports that optical identifications of NVSS radio sources produce a higher rate of radio loud NLS1s than optical selection (Whalen et al. 2001)

The reason for the scarcity of radio loud NLS1s is still unknown. Finding new radio loud NLS1s is thus of great importance for understanding the NLS1 phenomenon. According to Boroson & Green (1992), radio loudness in their quasar sample is closely linked to “eigenvector 1” in the sense that radio sources tend toward *small* values of FeII equivalent width and high [OIII] peak values (see also Marziani et al. 2001). The study of radio properties of NLS1s, in particular their radio loudness and radio variability, also allows us to re-address questions related to the orientation of the inner region of NLS1s. It was originally suggested that NLS1s are preferentially viewed face on (Osterbrock and Pogge 1985) and some evidence for and against this scenario has been presented since then. The orientation issue is important not only for its own sake, but also enters black hole mass and accretion rate estimates and consequently affects black hole mass – bulge mass relations of NLS1s and their cosmological implications (e.g. see the discussion in Collin & Kawaguchi 2004). Finding more radio loud NLS1s may also shed new light onto the radio loud – radio quiet dichotomy of AGN (e.g., Sulentic et al. 2003, McLure & Jarvis 2004, and references therein), one of the key unsolved problems in AGN physics.

Here, we report detection of the radio loud NLQSO SDSS J172206.03+565451.6, found in the course of a search for radio loud narrow-line AGN (Komossa et al. 2005) making use of tools developed for the German Astrophysical Virtual Observatory GAVO². SDSS J172206.03+565451.6 is exceptional in that it is only the fourth identified NLQSO, is the second-most radio loud, and shows other interesting properties including a high accretion rate and unusually low BH mass despite its radio loudness. In our terminology, we follow the classical distinction between narrow-line Seyfert 1 galaxy and narrow-line quasar according to absolute visual magnitude when referring to individual objects, but we will collectively speak of NLS1 galaxies when referring to class properties which then includes both, NLS1s and NLQSOs. A cosmology with $H_0=70$ km/s/Mpc, $\Omega_M=0.3$ and $\Omega_\Lambda=0.7$ is adopted throughout, unless noted otherwise.

In Section 2 we establish SDSS J172206.03+565451.6 as a radio loud object and present results from optical and X-ray spectroscopy, followed by a discussion in Section 3.

²<http://www.g-vo.org/portal/>

2. Radio, optical and X-ray observations of SDSS J172206.03+565451.6

2.1. Radio-loudness of SDSS J172206.03+565451.6

SDSS J172206.03+565451.6 at redshift $z=0.425$ was identified (Anderson et al. 2003, Williams et al. 2002) in the course of the SLOAN Digital Sky Survey (SDSS; e.g., York et al. 2000) and was detected as X-ray source during the *ROSAT* All-Sky Survey (RASS, Voges et al. 1999). It was classified as NLS1 (Williams et al. 2002) but little else is known about this galaxy.

SDSS J172206.03+565451.6 stuck out as exceptionally radio loud in a search for radio loud narrow-line AGN by cross-correlating the NLS1s in the “Catalogue of Quasars and AGN” (Veron-Cetty & Veron 2003) with different radio catalogues including the FIRST, NVSS, WENSS, SUMSS and other surveys (for cross-correlation techniques and results on the full sample see Komossa et al. 2005). SDSS J172206.03+565451.6 is detected in the NVSS, FIRST and WENSS survey (Tab. 1). The radio positions agree within $<1''$ (WENSS: within $2.5''$) with the optical position of the galaxy. No indications for radio variability are seen, comparing the FIRST and NVSS radio flux. Zhou et al. (2003) mentioned in passing the radio loudness of this galaxy but did not discuss it further.

SDSS J172206.03+565451.6 shows a large scatter in blue magnitude when comparing different epochs (Tab. 1), $\Delta m_B \simeq 2.1$ mag, strongly indicating that the variability is real. At faintest state, $m_{B2}=19.92$ mag. Using SDSS g' and r' magnitudes (Tab. 1), we obtain $m_{B_{SDSS}}=18.46$ with the color transformation according to Smith et al. (2002).

Following the conventions of Kellermann et al. (1989), we calculate the radio index R as ratio of 6 cm radio flux to optical flux at 4400\AA . Under the assumption of similar spectral shapes in the optical and radio band with spectral index $\alpha = -0.5$ (Kellermann et al. 1989), $R = 10$ approximately marks the “border” between radio quiet and radio loud objects (which corresponds to a radio index at 1.4 GHz of $R_{1.4} = 1.9R$). For SDSS J172206.03+565451.6 we obtain $R_{1.4} = 100-700$, depending on choice of blue magnitude m_{B1} and m_{B2} from the USNO-B1 catalogue (Tab. 1), and after carrying out a Galactic extinction correction of $A_B=0.11$ mag. This puts SDSS J172206.03+565451.6 well above the threshold commonly used to call an object radio loud.

2.2. Optical spectroscopy

In order to confirm the optical spectral classification of SDSS J172206.03+565451.6, and to measure its continuum and emission-line properties, we analyzed the SDSS spectrum of

this galaxy. The Third Data Release (DR3, Abazajian et al. 2005) processed spectrum was used³. This spectrum is flux- and wavelength-calibrated by the spectroscopic pipeline in the course of the DR3 processing. We further applied a Galactic extinction correction to the spectrum, using $E_{B-V}=0.026$ mag (Schlegel, Finkbeiner & Davis 1998) and a standard $R=3.1$ extinction law. The IRAF package SPECFIT (Kriss 1994) was used for spectral analysis.

The spectrum of SDSS J172206.03+565451.6 is AGN dominated. We fit a single power law to the underlying continuum using the "continuum windows" known to be relatively free from strong emission lines at 3010-3040, 3240-3270, 3790-3810, 4200-4230, 5080-5100, 5600-5630, 5970-6000, and 6005-6035 Å (Forster et al. 2001, Vanden Berk et al. 2001). The continuum is well represented by a single powerlaw with index $\alpha = -1.38$ (Fig. 1), where $f_\lambda \propto \lambda^{+\alpha}$, except at highest energies around MgII, where the continuum level is slightly overpredicted.

The optical-UV spectrum shows emission from FeII complexes. An FeII spectrum, using the technique and optical FeII template described in Boroson & Green (1992), was first fitted and subtracted (excluding the UV FeII multiplets around MgII λ 2798, not included in the template).

More than 10 emission-lines are clearly present in the spectrum, including MgII2798, [NeV]3426, [NeIII]3869, [OII]3727, [OIII]5007 and Balmer lines. The FeII- and continuum-subtracted spectrum was used to measure emission line parameters (and a more appropriate local continuum around MgII2798 was specified to measure that line). Emission lines were fit by single- or multi-component Gauss and/or Lorentz profiles and emission-line widths and emission-line ratios were measured. Results are listed in Tab. 2. Line-widths were corrected for the instrumental broadening. The SDSS pipeline provides the resolution at every pixel. The instrumental response of relevant emission-lines in the spectrum is in the range of $\text{FWHM}_{\text{inst}} = 133 - 178$ km/s. It was corrected for in all FWHMs reported below.

Most weak lines are similarly well fit by either a Gaussian or Lorentzian line profile. In Tab. 2, therefore generally only results from the Gaussian fits are reported, plus results from direct measurements of line widths and line fluxes (without any assumption on line profile shape). The profiles of MgII, [OIII] and H β appear more complex. [OIII] λ 5007 shows an asymmetric broad wing frequently observed in NLS1 galaxies (e.g., Xu et al. 2003). The profile is well matched by two Gaussian components (Tab. 2) the peaks of which show a relative shift of 144 km/s. A direct measurement of the full width at the half of the peak flux gives $\text{FWHM}_{[\text{OIII}]} = 425$ km/s. The profile of H β is best fit by a model consisting of

³data were retrieved at <http://cas.sdss.org/dr3/en/tools/explore/obj.asp>

two Gaussians⁴. A direct measurement of the line width provides $\text{FWHM}_{\text{H}\beta,\text{d}} = 1494\text{km/s}$.

In summary, SDSS J172206.03+565451.6 fulfills the classical optical criteria for classification as a NLQSO. In particular, $\text{FWHM}_{\text{H}\beta} \simeq 1494\text{ km/s}$ while $\text{FWHM}_{[\text{OIII}]}$ $\simeq 425\text{ km/s}$, and $I_{[\text{OIII}]\lambda 5007}/I_{\text{H}\beta_{\text{total}}} = 0.7$.⁵ The ratio of $\text{FeII}\lambda 4570$ to $\text{H}\beta_{\text{total}}$ amounts to 0.7, where the FeII blend is measured between 4434\AA and 4684\AA .

The radio loudness of SDSS J172206.03+565451.6 can be re-evaluated by using the optical flux at 4400\AA restframe obtained from the SDSS spectrum and the 5 GHz restframe radio flux predicted from the actually observed radio spectral index $\alpha_{r_{1.4-0.33}} = -0.69$ ($f_\nu \propto \nu^\alpha$). α_r was calculated from the radio observations at 1.4 (FIRST) and 0.33 GHz (Tab. 1) assuming that no spectral break occurs in between. This then gives $R_{5\text{GHz}}=360$ and re-confirms the radio loudness of SDSS J172206.03+565451.6.

2.3. X-ray spectroscopy and variability

SDSS J172206.03+565451.6 was detected in X-rays during the RASS. We analyzed these data in order to check for variability and to measure the spectral shape (pointed observations with *ROSAT* or any other X-ray mission are not available). Standard procedures of data reduction were followed. Source photons were extracted from a circular region centered on the source position. The background was determined in two source-free areas along the scan direction of the X-ray telescope. Data were corrected for vignetting.

We find that the spectrum can be well fit by a single powerlaw, but powerlaw index and amount of absorption are not well constrained. If absorption is treated as free parameter, we obtain $N_{\text{H}} \simeq 0.45 \times 10^{21}\text{ cm}^{-2}$ and $\Gamma_x \simeq -3.0$ ($\chi^2_{\text{red}}=0.4$), while for $N_{\text{H}}=N_{\text{Gal}}=0.16 \times 10^{21}\text{ cm}^{-2}$ we find $\Gamma_x \simeq -2.1$ ($\chi^2_{\text{red}}=0.5$). The absorption-corrected (0.1–10) keV flux obtained for these two models is uncertain by a factor ~ 2 and converts into an X-ray luminosity of $L_{(0.1-10)\text{keV}} \simeq (1 - 2) \times 10^{45}\text{ erg/s}$. More complex models than simple powerlaws are not warranted, given the faintness of the source (~ 115 source photons detected).

⁴There is some ongoing discussion as to which profiles are the best representation of the complex AGN emission line shapes (e.g., Veron-Cetty et al. 2001, Sulentic et al. 2002). In the present work, we applied both, combinations of Gaussians and Lorentzians to the line profiles. We find that ultimately the profile of H β is best represented by two Gaussians. However, explicit choice of line profile does not have any further consequences for our study, since derived line ratios and FWHMs for the brighter emission lines agree within typically $\sim 30\%$ of each other, independent of profile choice. The classification of SDSS J172206.03+565451.6 as a NLS1 is unaffected.

⁵The "direct" measurements ("d") of Tab. 2 are quoted here, since they are the most model-independent.

We also inspected the X-ray lightcurve of SDSS J172206.03+565451.6 and find that its X-ray emission is constant within the errors throughout the RASS observation.

3. Discussion

3.1. Radio properties of SDSS J172206.03+565451.6 and comparison with other radio loud NLQSOs

We have shown that SDSS J172206.03+565451.6 fulfills all criteria for classification as a NLQSO and is one of the radio loudest NLQSOs known. This does not only hold for radio index, but also for radio power. We obtain $P_{1.4} \simeq 3 \times 10^{25}$ W/Hz, significantly within the radio loud regime ($P_{4.85} > 10^{24}$ W/Hz, Joly et al. 1991). In particular, this is also orders of magnitude above the most radio-luminous starbursts studied by Smith et al. (1998) which have $\log P_{4.85,SB} \simeq 22.3 - 23.4$ W/Hz. This excludes the possibility that the radio emission of SDSS J172206.03+565451.6 is starburst-dominated. Also, we measured the ionization parameter for SDSS J172206.03+565451.6 from [OII]/[OIII] which is in a regime typical of Seyfert galaxies (next Section).

The radio spectral shapes of the few known radio loud NLQSOs appear to scatter widely, with $\alpha_{2.7,4.85\text{GHz}} = 0.6$ (SDSS J094857.3+002225, Zhou et al. 2003), $\alpha_{4.85,8.4\text{GHz}} = -1.4$ (RXJ0134-4258, Grupe et al. 2000), and $\alpha_{0.33,1.4\text{GHz}} = -0.7$ (SDSS J172206.03+565451.6), while the NLS1-like galaxy PKS 2004-447 shows $\alpha_{\text{ATCA}} = -0.6$ (Oshlack et al. 2001) where $f_\nu \propto \nu^\alpha$. It has to be kept in mind, though, that they were measured at different frequencies and are generally based on non-simultaneous observations.

While PKS0588-504 is highly variable in the X-ray band on various time scales (e.g., Gliozzi et al. 2001), and RXJ0134-4258 dramatically changed its spectral shape (Grupe et al. 2000, Komossa & Meerschweinchen 2000), little can be said on the longer-term X-ray variability properties of SDSS J172206.03+565451.6 based on the short RASS observation. Dedicated X-ray observations of this galaxy will be useful to re-address this issue.

3.2. Emission-line diagnostics

We attempted to measure extinction by using the Balmer lines $H\beta$, $H\gamma$ and $H\delta$. However, at location of $H\delta$ the red and blue part of the SDSS spectrum were merged, and a bump underlying and redward of $H\delta$ implies its measurement is highly uncertain. Similarly, $H\gamma$ comes with some uncertainty, because the line is partially blended with [OIII]4363. The observed

value, $H\beta/H\gamma \simeq 0.28..0.46$, is uncertain by almost a factor of two, and within this uncertainty is consistent with the Case-B recombination value, 0.47. The absence of strong reddening of the spectrum is also hinted by the blue continuum exhibited by SDSS J172206.03+565451.6.

The emission-line ratio $[OII]\lambda 3727/[OIII]\lambda 5007$ is a good indicator of the ionization parameter U (Penston et al. 1990), as long as the emission-line region in question does not contain strong density inhomogeneities (Komossa & Schulz 1997). The ratio observed in SDSS J172206.03+565451.6, $\log [OII]/[OIII] \simeq -0.6$ (Tab. 2), implies $\log U \simeq -2.3... -2.6$ which is based on re-calculation of Fig. 7 of Komossa & Schulz (1997) but using typical NLS1 ionizing continua and a NLR cloud density in the range $\log n_H = 2 - 3$. The NLS1 continua are composed of the mean spectral energy distribution (SED) of the NLS1 NGC 4051 outside the EUV–X-ray regime plus a systematically varying additional EUV excess and varying steepness of the X-ray continuum spectrum (see caption of Fig. 2 for details). Photoionization calculations were carried out using the code *Cloudy* (Ferland et al. 1998) with assumption as in Komossa & Schulz (1997; in brief: ionization-bounded clouds of constant density and solar metallicity illuminated by a central point-like continuum source). Fig. 2a demonstrates that for NLS1-like continua, $[OII]/[OIII]$ is still a good diagnostic of ionization parameter, relatively independent of continuum shape⁶. The ionization parameter estimated for SDSS J172206.03+565451.6 is comparable to other Seyferts and in particular is similar to the NLS1 galaxy NGC 4051 ($\log U \simeq -2.2... -2.5$ applying the same method; Komossa & Fink 1997).

Examining other line ratios for their diagnostic value, we find that once the ionization parameter is known, the ratio of $[NeV]/[NeIII]$ is a very good diagnostic of the EUV-soft X-ray continuum, relatively independent of density (Fig. 2b). SDSS J172206.03+565451.6 is unusual in its relatively strong NeV emission which does indicate the presence of a high-energy continuum excess, i.e., a spectral energy distribution (SED) similar to continuum ‘c3’-‘c4’ (see Fig. 2).

Essentially all of the 128 NLQSOs listed in the “Catalogue of Quasars and AGN” compiled by Veron-Cetty & Veron (2003) have redshifts in a range where both $[OII]\lambda 3727$ and $[NeV]\lambda 3426$ are easily measurable by optical spectroscopy. The combination of the $[OII]/[OIII]$ and $[NeV]/[NeIII]$ diagrams is thus a very useful tool in estimating ionization parameters of NLS1s and constraining their EUV continua. These line-ratios should be a beneficial addition in sampling the “Eigenvector” parameter space of radio loud and radio quiet NLS1s, complementing line ratios such as $FeII/H\beta$ and line profiles shapes already in

⁶deviations arise for extreme soft excess continua and high ratios of $[NeV]/[NeIII]$ for which the method should be re-evaluated

use (e.g. Sulentic et al. 2003, Bachev et al. 2004).

3.3. Black hole mass and accretion rate

Using the $H\beta$ line width and X-ray luminosity of SDSS J172206.03+565451.6, we obtain an estimate of black hole mass and accretion rate in terms of the Eddington rate.

Assuming that the broad line region (BLR) clouds are virialized (e.g., Wandel et al. 1999), the black hole mass can be estimated as $M_{\text{BH}} = G^{-1} R_{\text{BLR}} v^2$. The BLR radius, R_{BLR} , can be determined from the optical luminosity at 5100\AA according to equation (6) of Kaspi et al. (2000), $R_{\text{BLR}} = 32.9 \left[\frac{\lambda L_{\lambda}(5100\text{\AA})}{10^{44} \text{erg/s}} \right]^{0.7} \text{ld}$ (derived for a cosmology with $H_0 = 75 \text{ km/s/Mpc}$ and $q_0 = 0.5$). The velocity v of the BLR clouds is usually estimated from the FWHM as $v = f \text{FWHM}$ where $f = \frac{\sqrt{3}}{2}$ for an isotropic cloud distribution. With $L_{\lambda}(5100\text{\AA})_{H_0=75, q_0=0.5} = 4.3 \times 10^{40} \text{ erg/s/\AA}$ derived from the SDSS spectrum, and $\text{FWHM}_{H\beta, d} = 1494 \text{ km/s}$, we obtain a black hole mass of $M_{\text{BH}} \simeq 1.9 \times 10^7 M_{\odot}$ for SDSS J172206.03+565451.6. More appropriately using the FWHM of the broad component from the two-component fit to $H\beta$, we get $M_{\text{BH}} \simeq 3.3 \times 10^7 M_{\odot}$.⁷

SDSS J172206.03+565451.6 falls right into an unpopulated regime of the ‘‘Laor diagram’’ (Fig. 2 of Laor 2000) which plots the relation between radio loudness and black hole mass. While larger samples filled up some originally empty areas in the Laor diagram (e.g., Lacy et al. 2001, Oshlack et al. 2001, 2002, Woo and Urry 2002, McLure & Jarvis 2004), SDSS J172206.03+565451.6 is still located in a region relatively sparsely populated. This either implies that SDSS J172206.03+565451.6 has an exceptionally low black hole mass given its radio properties, or that beaming is important in explaining its radio emission with the consequence that this NLQSO is seen face-on, and is thus an important cornerstone object for future studies of inclination effects in NLS1 galaxies (see Komossa et al. 2005 for further discussion).

With knowledge of BH mass and X-ray luminosity it is possible to make a rough estimate of the accretion luminosity relative to the Eddington value. According to Maccarone et al. (2003, and references therein), Galactic X-ray binaries in soft/high-state and AGN show *suppressed* radio emission for relatively high accretion rates, in the range of 0.01-0.1 times the Eddington rate. With $M_{\text{BH}} \simeq (1.9 - 3.3) \times 10^7 M_{\odot}$ and $L_{x,(0.1-10)\text{keV}} \simeq (1 - 2) \times 10^{45}$

⁷For comparison, Bian and Zhao (2004), who included SDSS J172206.03+565451.6 in a sample of galaxies for which they estimated BH masses, obtained $M_{\text{BH}} \simeq 2.3 \times 10^7 M_{\odot}$ based on a single-component direct measurement of $\text{FWHM}_{H\beta}$.

erg/s, we obtain $L/L_{\text{Edd}}=0.2-0.8$ *without* any bolometric correction which should typically be an additional factor 5–10 (Tab. 14 and 15 of Elvis et al. 1994). This estimate demonstrates that SDSS J172206.03+565451.6 accretes at a high rate and, in particular, that it exceeds the accretion rate at which radio emission is expected to be suppressed.

4. Summary

We have presented a study of the radio loud NLQSO SDSS J172206.03+565451.6. One of the radio loudest NLQSOs known, its combination of black hole mass and radio index put it into a scarcely populated region in $M_{\text{BH}}-R$ diagrams in that its black hole mass is unusually low given its radio loudness. Its Eddington ratio L/L_{Edd} is close to unity. Future searches for and study of similar objects may hold important clues to the nature of radio loud NLS1s in particular and NLS1 models in general, and the mechanism which causes the radio loud – radio quiet bimodality in AGN.

We thank Gary Ferland for providing *Cloudy*. GAVO is funded by the *Bundesministerium für Bildung und Forschung* (BMBF) under contract no. 05 AE2EE1/4. DX acknowledges the support of the Chinese National Science Foundation (NSF) under grant NSFC-10503005. This research made use of the SDSS and VizieR archives, the NED service, and the Guide Star Catalogue-II.

REFERENCES

- Abazajian, K., Adelman-McCarthy, J.K., Agüeros, M.A., et al., 2005, *AJ*, 129, 1755
- Anderson, S.F., Voges, W., Margon, B., et al., 2003, *AJ*, 126, 2209
- Bachev, R., Marziani, P., Sulentic, J.W., et al., 2004, *ApJ*, 617, 171
- Becker, R.H., Helfand, D.J., White, R.L., Gregg, M.D., & Laurent-Muehleisen, S.A., 2003, *VizieR On-line Data Catalog: VIII/71*
- Bian, W., & Zhao, Y., 2004, *MNRAS*, 347, 607
- Boroson, T.A., & Green, R.F., 1992, *ApJS*, 80, 109
- Botte, V., Ciroi, S., Rafanelli, P., Di Mille, F., 2004, *AJ*, 127, 3168
- Collin, S., & Kawaguchi, T., 2004, *A&A*, 426, 797

- Condon, J.J., Cotton, D., Greissen, E.W., et al., 1998, *AJ*, 115, 1693
- de Bruyn, G., Miley, G., Rengelink, R., et al., 1998, Westerbork Northern Sky Survey (WENSS), <http://www.strw.leidenuniv.nl/wenSS/>
- Elvis, M., Wilkes, B.J., McDowell, J.C., et al., 1994, *ApJS*, 95, 1
- Ferland, G.J., Korista K.T., Verner D.A., et al., 1998, *PASP*, 110, 761
- Forster, K., Green, P.J., Aldcroft, T.L., et al. 2001, *ApJS*, 134, 35
- Glozzi, M., Brinkmann, W., O'Brien, P.T., et al., *A&A*, 365, L128
- Greene, J.E., Ho, L.C., Ulvestad, J.S., 2005, *ApJ*, submitted
- Grupe, D., Leighly, K.M., Thomas, H.-C., & Laurent-Muehleisen, S.A., 2000, *A&A*, 356, 11
- Grupe, D., 2004, *AJ*, 127, 1799
- Grupe, D., & Mathur, S., 2004, *ApJ*, 606, L41
- Joly, M., 1991, *A&A*, 242, 49
- Kaspi, S., Smith, P.S., Netzer, H., et al., 2000, *ApJ*, 533, 631
- Kellermann, K.I., Sramek, R., Schmidt, M., Shaffer, D.B., & Green, R., 1989, *AJ*, 98, 1195
- Komossa, S., & Schulz, H., 1997, *A&A*, 323, 31
- Komossa, S., & Fink, H., 1997, *A&A*, 322, 719
- Komossa, S., & Meerschweinchen, J., 2000, *A&A*, 354, 411
- Komossa, S., et al., 2005, *AJ*, to be submitted
- Kriss, G.A., 1994, in: *ASP Conf. Ser. 61, ADASS III*, eds: D.R. Crabtree, R.J. Hanisch & J. Barnes (San Francisco: ASP), 437
- Lacy, M., Laurent-Muehleisen, S.A., Ridgway, S.E., et al., 2001, *ApJ*, 551, L17
- Laor, A., 2000, *ApJ*, 543, L111
- Maccarone, T.J., Gallo, E., & Fender, R., 2003, *MNRAS*, 345, L19
- Maccarone, T.J., Miller-Jones, J.C.A., Fender, R.P., & Pooley, G.G., 2005, *A&A*, in press

- Marziani, P., Sulentic, J.W., Zwitter, T., Dultzin-Hacyan, D., & Calvani, M., 2001, *ApJ*, 558, 560
- Mathur, S., 2001, *New Astronomy*, 6, 321
- Mathur, S., & Grupe, D., 2005, *ApJ*, in press
- McLure, R.J., Jarvis, M.J., 2004, *MNRAS*, 353, L45
- Monet, D.G., Levine, S.E., Canzian, B., et al., 2003, *AJ*, 125, 984
- Moran, E., 2000, *New Astronomy Reviews*, 44, 527
- Oshlack, A.Y.K.N., Webster, R.L., & Whiting, M.T., 2001, *ApJ*, 558, 578
- Oshlack, A.Y.K.N., Webster, R.L., & Whiting, M.T., 2002, *ApJ*, 576, 81
- Osterbrock, D.E., & Pogge, R., 1985, *ApJ*, 297, 166
- Penston, M.V., Robinson, A., Alloin, D., et al., 1990, *A&A*, 236, 53
- Pounds, K., Done, C., & Osborne, J.P., 1995, *MNRAS*, 277, L5
- Remillard, R.A., Bradt, H.V., Buckley, D.A.H., et al., 1986, *ApJ*, 301, 742
- Schlegel, D.J., Finkbeiner, D.P. & Davis, M., 1998, *ApJ*, 500, 525
- Siebert, J., Leighly, K.M., Laurent-Muehleisen, S.A., et al., 1999, *A&A*, 348, 678
- Simkin, M.V., & Roychowdhury, V.P., 2003, *Complex Systems* 14, 269
- Smith, D.A., Herter, T., & Haynes, M.P., 1998, *ApJ*, 494, 150
- Smith, J.A., Tucker, D.L., Kent, S., et al., 2002, *AJ*, 123, 2121
- Sulentic, J.W., Marziani, P., Zamanov, R., et al., 2002, *ApJ*, 566, L71
- Sulentic, J.W., Zamfir, S., Marziani P., et al., 2003, *ApJ*, 597, L17
- Ulvestad, J.S., Antonucci, R.R.J., & Goodrich, R.W., *AJ*, 109, 81
- Vanden Berk, D.E., Richards, G.T., Bauer, A., et al., 2001, *AJ*, 122, 549
- Veron-Cetty, M.P., & Veron, P., 2000, *A&ARv*, 10, 81
- Veron-Cetty, M.P., Veron, P., & Goncalves, A.C. 2001, *A&A*, 372, 730

- Veron-Cetty, M.P., & Veron, P., 2003, *A&A*, 412, 399
- Voges, W., Aschenbach, B., Boller, T., et al., 1999, *A&A*, 349, 389
- Wandel, A., Peterson, B.M., & Malkan, M.A., 1999, *ApJ*, 526, 579
- Wang, J.-M., Netzer, H., 2003, *A&A*, 398, 927
- Whalen, J., Laurent-Muehleisen, S.A., Moran, E.C., & Becker, R.H., 2001, *BAAS* 33, 1373
- Williams, R.J., Pogge, R.W., & Mathur, S., 2002, *AJ*, 124, 3042
- Woo, J.-H., & Urry, M.C., 2002, *ApJ*, 579, 530
- Xu, D., Komossa, S., Wei, J., Qian, Y., & Zheng, X.Z., 2003, *ApJ*, 590, 73
- York, D.G., et al., 2000, *AJ*, 120, 1579
- Zhou, H.-Y., Wang, T.-G., Dong, X.-B., Zhou, Y.-Y., & Li, C., 2003, *ApJ*, 584, 147

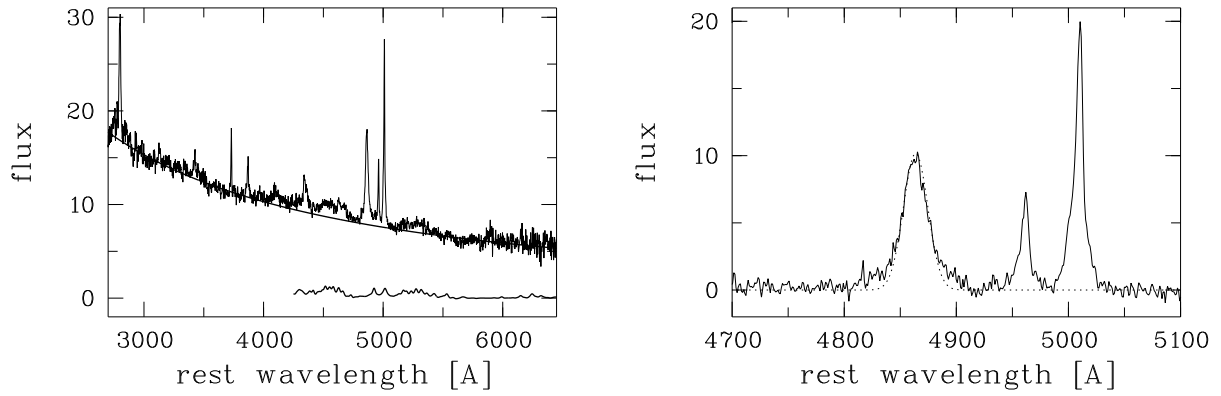


Fig. 1.— Left: Optical spectrum of SDSS J172206.03+565451.6 (flux f_λ in arbitrary units) and best-fit power-law continuum. The brightest lines are marked. The spectrum is shifted to the rest frame wavelength and smoothed with a boxcar of 3 pixels for clarity. The lower curve shows the best-fit FeII emission contribution. Right: Zoom onto the H β -[OIII] complex. The dashed line shows a single-Gaussian representation of H β .

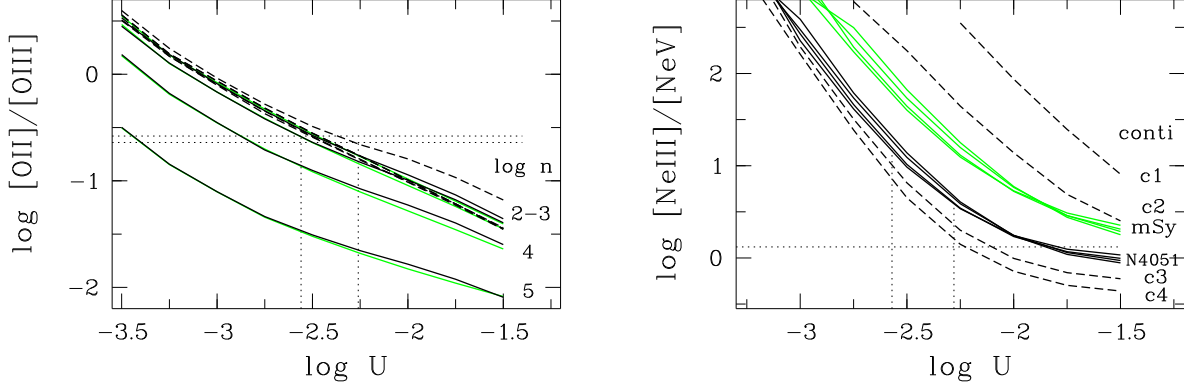


Fig. 2.— Left: The dependence of the emission-line ratio $[\text{OII}]3727/[\text{OIII}]5007$ on the ionization parameter U for different continuum shapes and cloud gas densities. The density varies from top to bottom between $\log n = 2-5$, as marked. The different continuum shapes lead to a very similar variation in $[\text{OII}]/[\text{OIII}]$ and we do not label them individually (the black solid line corresponds to the multi-wavelength spectral energy distribution (SED) of the NLS1 galaxy NGC 4051 (Komossa & Fink 1997) while the dashed line was calculated for NGC 4051-like continua with varying strength of an EUV–soft-X-ray excess, and the grey line was calculated for a mean Seyfert continuum). Models with $\log n = 4,5$ were not recalculated for all continuum shapes. The dotted line marks the measured $[\text{OII}]/[\text{OIII}]$ ratio with its uncertainty.

Right: The dependence of the emission line ratio $[\text{NeV}]3426/[\text{NeIII}]3869$ on U for different continuum shapes and gas densities. Line style coding is the same as for the $[\text{OII}]/[\text{OIII}]$ diagram. In addition, the continuum shape is indicated at the right-hand side of the figure. Models c1 to c4 correspond to NGC 4051-like SEDs except that the flux at $\log \nu = 16.383$ Hz, connected by powerlaws to the flux at the Lyman limit and to the flux at $\log \nu = 19.383$ Hz, was systematically increased – by factors of 0.04 (= EUV deficit rather than excess), 0.1, 3 and 7 for c1-c4, respectively – in order to describe soft excesses of varying strength. This then also changed the powerlaw indices α_{EUV} and α_x while the remainder of the SED was kept constant. Models involving the SED of NGC 4051 itself or a mean Seyfert ‘mSy’ SED were re-calculated for densities ranging between $\log n = 2-4$. Individual densities are not marked in the plot since it can be seen that the density dependence is very weak.

Table 1: Properties of SDSS J172206.03+565451.6. Flux/magnitude estimates are based on the following catalogues: USNO (Monet et al. 2003), GSC 2.2, SDSS (Anderson et al. 2003), FIRST (Becker et al. 2003), NVSS (Condon et al. 1998), and WENSS (de Bruyn et al. 1998).

waveband	flux/brightness	catalogue and comments
m _{B1}	17.8 mag	USNO-B1.0
m _{B2}	19.9 mag	USNO-B1.0
m _{Bj}	18.66 mag	GSC 2.2
u'	18.65 mag	SLOAN
g'	18.35 mag	SLOAN
r'	18.26 mag	SLOAN
i'	18.07 mag	SLOAN
z'	17.93 mag	SLOAN
1.4 GHz	39.8 mJy	FIRST
1.4 GHz	42.6 mJy	NVSS
0.33 GHz	108 mJy	WENSS
X-rays, (0.1–10) keV	1.5..3.6 10 ⁻¹² *	this paper

*absorption-corrected flux in erg cm⁻² s⁻¹ Hz⁻¹ (see Sect. 2.3 on models).

Table 2: Optical-UV emission lines of SDSS J172206.03+565451.6. The second column, labeled “m”, refers to the method the line width and flux was measured (g = Gaussian profile fit, l = Lorentzian, d = direct integration over the observed profile, without any model assumption, g+g = two component Gaussian of which narrow and broad component are reported in separate rows).

line identification	m	line ratio	FWHM _c [km/s]	comment
[OIII] λ 5007	g	0.57	487	
	d	0.75	425	
[OIII] _{narrow}	g+g	0.22	262	
[OIII] _{broad}	g+g	0.54	1044	
H β	g	0.94	1577	underpredicts broad wings (Fig. 1)
	l	1.31	1476	overpredicts flux in the wings
	d	1.11	1494	
H β _{total}	g+g	1.0!		
H β _{narrow}	g+g	0.05	425!	FWHM _{Hβ_{narrow}} fixed to FWHM _{[OIII]_d}
H β _{broad}	g+g	0.95	1980	
FeII 4570		0.73		
[NeIII] λ 3869	g	0.09	429	
	d	0.10:	415	
[OII] λ 3727	g	0.15	418	
	d	0.17	495	
[NeV] λ 3426	g	0.08	599	
	g	0.07	429!	FWHM _[NeV] fixed to FWHM _{[NeIII]_g}
MgII λ 2796+2803	g	0.80	1684	
	d	0.87	1433	